PCCP

Accepted Manuscript

ROYAL SOCIETY OF CHEMISTRY

www.rsc.org/pccp

First principles study of magnetoelectric coupling in $Co_2FeAl/BaTiO_3$ tunnel junctions

Li Yu[a,b], Guoying Gao[a], Lin Zhu[a], Lei Deng[b], Zhizong Yang[b], Kailun Yao[a,*]

[a]School of Physics and Wuhan National High Magnetic Field Center, Huazhong University of Science and Technology, Wuhan 430074, China

[b]Department of Basics, Air Force Early Warning Academy, Wuhan 430019, China

*Corresponding author at: School of Physics and Wuhan National High Magnetic Field Center, Huazhong University of Science and Technology, Wuhan 430074, People's Republic of China. Tel.: +86 27 87558523; fax: +86 27 87556264.

E-mail addresses: klyao@mail.hust.edu.cn (Kailun Yao).

Abstract

Critical thickness for ferroelectricity and magnetoelectric effect of $Co_2FeAl/BaTiO_3$ multiferroic tunnel junction (MFTJ) are investigated using the first-principles calculations. The ferroelectric polarization of the barriers can be maintained until a critical thickness of 1.7 nm for both the Co_2/TiO_2 and $FeAl/TiO_2$ interfaces. The magnetoelectric effect is derived from the difference of the magnetic moments on interfacial atoms, which is sensitive to the reversal of electric polarization. The magnetoelectric coupling is found to be dependent on the interfacial electronic hybridizations. Compared with the Co_2/TiO_2 interface, more net magnetization change is achieved at the $FeAl/TiO_2$ interface. In addition, the in-plane strain effect shows that in-plane compressive strain can lead to the enhancement of ferroelectric polarization stability and intensity of magnetoelectric coupling. These findings suggest that $Co_2FeAl/BaTiO_3$ MFTJ could be utilized in the area of electrically controlled magnetism, especially the MFTJ with loaded in-plane compressive strain with $FeAl/TiO_2$ interface.

Keywords: Ferroelectric; Magnetoelectric effect; Strain; First-principles

1. Introduction

Multiferroics are materials which exhibit two or more types of ferroic order simultaneously, including ferromagnetic (FM), ferroelectric (FE), ferroelastic, or ferrotoroidic. One of the most important characteristics of multiferroic materials is magnetoelectric (ME) properties, originating from the coupling between FE and FM order parameters.[1,2] This magnetoelectric materials are of great scientific and technological interest and could yield novel application designs.[3,4] There are several mechanisms resulting in ME effects, and the recent reviews can be seen in Refs. 5-7. Besides the intrinsic ME coupling occurs in compounds with no time-reversal and no space-inversion symmetries, much efforts have focused on the so called "interfacial magnetoelectricity" in which the ME coupling arises as an extrinsic effect at the interface of artificial composite multiferroics, such as the MFTJs, which refer to magnetic tunnel junctions (MTJs) with FE barriers or the ferroelectric tunnel junctions (FTJs) with FM electrodes,[8,9] allowing magnetic (electric) controls of ferroelectric (magnetic) properties. The control and utilization of the charge and spin degrees of freedom in spintronic devices has been an attractive issue in recent years, but the actual application of MFTJs face a number of challenges. The first challenge is that the decreasing thickness of FE barrier layer in a MFTJ will induce the degradation of ferroelectric polarization. It has long been believed that the critical size for ferroelectricity is more than a few tens of nanometers. However, recent studies demonstrated the electric polarization of ferroelectric thin films can be stabilized in several nanometers. Experimentally, a critical thickness of 3.5 nm has been measured in $BaTiO_3$ at 77 K.[10] Theoretically, Junquera et al. reported that the ferroelectric critical thickness of $BaTiO_3$ is as low as ~24 Å by using $SrRuO_3$ electrode.[11] Obviously, the screening effects of metal electrodes play an important role in lowing the critical thickness for ferroelectricity in MFTJs. The other challenge is to maintain high ME coupling between FM electrodes and FE barrier in MFTJs. In the MFTJs, two interfacial ME coupling mechanisms have been recently proposed,[12-13] namely the interface chemistry mechanism and the spin-dependent electrostatic screening mechanism. The interface chemistry mechanism is predicted that displacements of atoms at the FM/FE interface caused by ferroelectric instability alter the chemical

bonding and the hybridization at the interface which affects the interface magnetization. It is expected to play an important role in many interfaces, for example, $Fe/BaTiO_3$, $Co_2MnSi/BaTiO_3$, $Fe_3O_4/BaTiO_3$, etc.[12,14-18] For the latter, An applied electric field produces an accumulation of spin-polarized electrons or holes at the FM/FE interface resulting in a change in the interface magnetization, for example, $SrRuO_3/BaTiO_3$, $La_{1-x}Sr_xMnO_3/BaTiO_3$, etc.[19-22] Experimentally, the spin-dependent electrostatic screening ME coupling was also found in the $PbZr_{0.2}Ti_{0.8}O_3/La_{0.8}Sr_{0.2}MnO_3$ junction.[23] In addition, an asymmetric MFTJ can also provide a large ME coupling effect. [24-27] So far, our discussion of ME coupling has ignored the effects of strain. In multiferroic composites, the strain induced in one component (either by magnetostriction in the magnet under an applied magnetic field or by inverse piezoelectric effect in the ferroelectric under an applied electric field) can be mediated to the other and alters its polarization (be it electric or magnetic). Hence, this allows one to control the electric polarization of the composite by a magnetic field or its magnetization by an electric field. It is addressed as "strain-mediated magnetoelectric effect" in previous work.[28] This strain can largely affect the ME coupling in multiferroic composites.[29,30] In addition, enormous strains can also exist in thin films when one material is deposited on another, resulting from differences in crystal lattice parameters. The electronic properties of the FE layer are very sensitive to the external strain.[31,32] Therefore, it is expected to have an important effect on the ME coupling in MFTJs in our paper.

Here, we present a $Co_2FeAl/BaTiO_3$ layered nanostructure as a half-metallic/ferroelectric junction showing remarkable ME effects. Due to the excellent properties-high magnetic moments of 5μB per f.u.,[33] a high Curie temperature of 1000 K, half-metallic behavior, giant tunnelling magneto-resistance (330% at room temperature)[34, 35] and magnetic anisotropy[36,37]—the Heusler compound, Co_2FeAl, has been used as an attractive magnetic material in spin dependent electronic devices. But the multiferroic tunnel junctions formed by it and ferroelectric materials have never been studied. The critical thickness for ferroelectricity and magnetoelectric effect in $Co_2FeAl/BaTiO_3$

MFTJ is what we are interested in this paper. It is known that Co_2FeAl may be in a perfect chemically ordered $L2_1$ phase, or B2 phase and A2 phase. In the past, the investigated Co_2FeAl films reported in the literatures were mostly in B2 phase[34] and the totally ordered phase ($L2_1$) was difficult to achieve. Recently, Qiao et al. prepared the Co_2FeAl film with $L2_1$ structure using molecular beam epitaxy (MBE) technique with a certain temperature.[36] This structure was also obtained in Refs. 37, 38. Here, the Co_2FeAl that we considered is the $L2_1$ structure. The $BaTiO_3$ is a prototypical perovskite-like FE oxide, which also shows high Curie temperature 400 K. These two materials have a good match of lattice constants with each other between Co_2FeAl (110) and $BaTiO_3$ (100), the mismatch is about 1.5% that could be negligible.

In the present paper, we have investigated the critical thickness of $BaTiO_3$ barrier and ME effect in $Co_2FeAl/BaTiO_3$ MFTJ based on density functional theory. The ferroelectric polarization of the barriers can be maintained until a critical thickness of 1.7 nm for both the Co_2/TiO_2 and $FeAl/TiO_2$ interfaces. The ME coefficient calculated for these two interfaces are different from each other. A larger ME coefficient are achieved at the $FeAl/TiO_2$ interface compared with the Co_2/TiO_2 interface. In addition, the biaxial in-plane strain which can be achieved by epitaxial growth of $Co_2FeAl/BaTiO_3$ tunnel junction on different substrates have also been considered. We have shown that the in-plane compressive strain can lead to the enhancement of ferroelectric polarization stability and intensity of magnetoelectric coupling.

2. Computational details

First-principles calculations based on the density functional theory (DFT) are performed to investigate the electronic and atomic structure of $Co_2FeAl/BaTiO_3$ MFTJ using the Vienna Ab-initio Simulation Package (VASP).[39,40] To treat electron exchange and correlation, we choose the Perdew–Burke–Ernzerhof form[41] of generalized gradient approximation (GGA). Based on the early report,[42] simple GGA calculations are insufficient to

explain the electronic properties of Co_2FeAl, the GGA+U method is used to consider on-site correlation of 3d transition metals. The effective Coulomb-exchange interaction $U_{\text{eff}} = U - J$ is used, where U and J are the Coulomb part and the exchange part, respectively. A $U_{\text{eff}} = 2.2\text{eV}$ for Co atoms and $U_{\text{eff}} = 2.1\text{eV}$ for Fe atoms are applied in our calculations.[42] The cutoff energy of the plane waves is chosen to be 500 eV, which is large enough to deal with all the elements considered here with the PAW method. Atomic relaxations are performed using a 6×6×1 Monkhorst-Pack k-point sampling[43] and the ions are relaxed until the forces on each ion are less than 10 meV/Å. Subsequent, the grid is increased to 12×12×1 for electronic structure calculations. The spin-orbit interaction is not included in our calculations since its influence is expected to be very small for 3d elements.

In this paper, the $Co_2FeAl/BaTiO_3$ supercells are built up by stacking the bulk Co_2FeAl periodically along the [0 0 1] direction with $BaTiO_3$ layers terminated by TiO_2 layers, which is believed to be $BaTiO_3$'s most stable termination with magnetic materials.[12,44] In order to study the ME coupling's dependence on interface configuration, Co_2 and FeAl interfaces in the Co_2FeAl layer are simulated. Here, all the calculations with periodic boundary conditions are along the a, b and c-axis. Because the $BaTiO_3$ is known experimentally to have a tetragonal ferroelectric phase with spontaneous polarization along [001] direction at room temperature,[45] we have only discussed the polarization along c-axis. Considering the typical soft-mode distortion of bulk $BaTiO_3$, the initial ferroelectric displacements between Ti and O atoms at each TiO_2 layer is artificially set to be 0.125Å for the atomic relaxation. For the unstrained MFTJ, the in-plane lattice constant is fixed to be the experimental value of the bulk $BaTiO_3$ (3.991Å), while the out plane (z) lattice parameter c of the superlattice is optimized. Under the in-plane constraint, we find that the polarization of the bulk $BaTiO_3$ is 0.31C/m^2, as calculated using Berry's phase method,[46] while the magnetic moment of Co and Fe atom are 1.17 μ_B and 3.07 μ_B in the bulk Co_2FeAl, respectively, which is in agreement with the previous report.[47] In addition, the biaxial in-plane strain is implemented by adjusting the in-plane lattice constant, which is defined as $\eta = (a_s - a_0)/a_0$, where a_s and a_0 are the in-plane lattice constants of

strained and unstrained MFTJ, respectively. And the out-of plane lattice constant is allowed to be relaxed for each strain value during the geometry optimizations.

In order to determine the atomic relative positions at interface, the free energy of PE superlattices are tested for the $Co_2FeAl/BaTiO_3$ (001) interface with the same interfacial compositions but different atomic positions. We found that the TiO_2-terminated surface with inerfacial O atoms lying on top of the M (M=Co, Fe) atom is the most stable and energetically favorable, which is consistent to the previous studies.[12,17,44] Within a supercell, the Co_2FeAl slab is composed of 9 atomic layers for $FeAl/TiO_2$ interface and of 11 atomic layers for Co_2/TiO_2 interface. And for the $BaTiO_3$ slab, various thicknesses were considered, so that our supercells can be constructed as $(Co_2FeAl)_5$-Co_2/TiO_2-$(BaO\text{-}TiO_2)_m$ and $(Co_2FeAl)_4$-$FeAl/TiO_2$-$(BaO\text{-}TiO_2)_m$, where m=2, 4, 6, 8. The atomic structures of the m=6 multilayer are depicted in Fig. 1, and the ferroelectric polarization orientation is set to point to the right. Because of the symmetry of the constructed supercells, it allows us to study the effect of polarization reversal by comparing the properties of the left and right interfaces.

3. Results and discussion

First, we focus on the critical thickness of ferroelectricity in the unstrained $Co_2FeAl/BaTiO_3$ MFTJ. As is well-known, Ferroelectricity in BaTiO3 is mainly due to the local dipole set up by Ti-O distortions. So we calculate the relative Ti-O displacements of the $BaTiO_3$ multilayer for different thickness of the $BaTiO_3$ multilayer m value, as shown in Fig. 2. In both Co_2/TiO_2 and $FeAl/TiO_2$ interfaces, for m=2, it is found that the position of Ti atoms can spontaneously return the symmetry positions even if the symmetry equlilibrium is broken artificially, implying the $BaTiO_3$ layer maintains a paraelectric state.

For $m \geq 4$, as is seen from Figs. 2(a) and (b), the ferroelectric polarizations are significantly different from each other for the Co_2/TiO_2 and $FeAl/TiO_2$ interfaces. In the Co_2/TiO_2 interface, the relative Ti-O displacements are

all positive. In other words, the FE polarization becomes dominant and very O atom is displaced in the same direction for m ≥ 4 multilayers. But in the FeAl/TiO_2 interface, because of the larger covalent radius of Fe with respect to Al atom, the bond length between O and Fe atoms is comparably larger (2.032 Å for m=6, left interface; 2.037 Å for m=6, right interface) than that between O and Al atoms(1.851 Å and 1.864 Å for the same structure). Therefore, the O near the Fe is displaced away from the interface while the O near the Al is displaced toward the interface. The O atoms at both left and right interfaces are pinned down. At the left interface, the relative Ti-O_1 displacement induced by the interface bonding is about 0.31 Å (when m=6 or m=8), which is two times larger than the FE Ti-O displacement pattern in bulk $BaTiO_3$, while the relative Ti-O_2 displacement is 0.16 Å. (The positions of O_1, O_2, Co_1 and Co_2 atoms are marked in Fig. 1.) But at the right interface, the relative displacement is only 0.23 Å and 0.08 Å for Ti-O_1 and Ti-O_2, respectively. In other words, the Ti-O FE displacement pattern at the left interface makes larger electric dipoles of the interfacial TiO_2 atomic layer than the right interface. As a result, although the latter is divided into two regions with different thicknesses with oppositely oriented polarization, there is an overall net polarization in the insulating side. Therefore, although the special pattern of Ti-O FE displacement at FeAl/TiO_2 interface is remarkably different compared with that at the Co_2/TiO_2 interface, the ferroelectric polarization of the barriers can be maintained until a critical thickness of 1.7 nm (m=4) in both systems, which is consistent with the previous reports in similar systems.[12,15]

In the MFTJs, the polarization of ferroelectric thin film is affected significantly by the screening effect of metal electrode. The polarization of ferroelectric thin film leads to surface charges of opposite sign at the interfaces with the electrodes. Electrons in the metal tend to screen these charges, but perfect screening is not achieved, resulting in a sizeable depolarizing. The depolarization field attributing to the incomplete screening is usually pointing antiparallel to the spontaneous polarization, which becomes larger in thinner barriers,[48] and below the critical thickness, the depolarization field will be large enough to counteract completely the spontaneous

polarization of the $BaTiO_3$ layers. Then the system only shows PE state. The thicker the ferroelctric layer, the weaker the depolarization field. Therefore for the thick $BaTiO_3$ multilayers (m≥4), the system shows FE state.

Next, we turn to a discussion of the magnetic properties of the $Co_2FeAl/BaTiO_3$ MFTJ. Table 1 lists the magnetic moments of the atoms at the left and right interfaces for the Co_2/TiO_2 and $FeAl/TiO_2$ interfaces in case of m=6. Ferroelectric displacements break the symmetry between the left termination and right termination, causing magnetic moments of the interface metal atoms at the two interfaces to deviate from their values in the paraelectric state. In the Co_2/TiO_2 interface, the difference between the total magnetic moments of Co atoms at the two interfaces is $\Delta\mu_{Co} = -0.019\mu_B$, a larger difference $\Delta\mu_{Ti} = 0.156\mu_B$ occurs for Ti atoms. In the $FeAl/TiO_2$ interface, The net change of the magnetic moments at the interface is $\Delta\mu_{Fe} = 0.032\mu_B$ for Fe atoms and $\Delta\mu_{Ti} = 0.15\mu_B$ for Ti atoms when the electric polarization reverses. For both the Co_2/TiO_2 and $FeAl/TiO_2$ interfaces, it is seen that the induced magnetic moments of Ti atoms are all antiparallel to those of their neighboring Fe or Co atoms.

As we know, the different magnetic moments at the two interfaces represent the variation arising at one interface during the reversion of the polarization in the $BaTiO_3$. Similar to previous work, we estimate the ME coefficient α_s (a figure of merit for the ME coupling) of this multiferroic bilayer, which is defined as[12,49]

$$\mu_0 \Delta M = \alpha_s E$$

where ΔM is the net difference in total magnetic moments between two interfaces per unit area and E is the strength of the applied electric field. Although the effect predicted here is nonlinear due to the hysteretic dependence of the polarization on the electric field, we can still use α_s as a figure of merit for the ME coupling.[15-22] The polarization of $BaTiO_3$ is assumed to be switched at the coercive field of $E = E_C = 100\mathrm{Kv/cm}$. Taking into account that $\Delta M = 0.12\mu_B$ per unit area for Co_2/TiO_2 interface and $\Delta M = 0.18\mu_B$ per unit area for the $FeAl/TiO_2$ interface, respectively, we can obtain the surface ME coefficient $\alpha_s = 0.8\times10^{-10}\mathrm{Gcm^2/V}$ for

Co_2/TiO_2 interface and $\alpha_s = 1.3\times10^{-10}\,\mathrm{Gcm^2/V}$ for the $FeAl/TiO_2$ interface. It is obvious that the magnitude of α_s at the $FeAl/TiO_2$ interface is larger than that at the Co_2/TiO_2 interface.

To gain an insight into the nature of the induced interface magnetic moments, the projected density of states (PDOS) of Co_1 3d, Co_2 3d , Ti 3d orbitals at the Co_2/TiO_2 interface and Fe 3d, Al 3p and Ti 3d orbitals at the $FeAl/TiO_2$ interface are shown in Fig. 3. The electronic structures indicate that the center layer Co_2FeAl presents an approximate half-metallicity, instead of a perfect half-metallicity, mainly because of the insufficient thickness. And it is consistent with previous reports.[37] (i) In the Co_2/TiO_2 interface [see Fig. 3(a)], the Co_1 and Co_2 states are different, and they are also different from the bulk state, because of the exchange splitting of Co 3d states, the magnetic moments of the interfacial Co_1 and Co_2 atoms at the interface are larger than those in bulk. At the right interface, appreciable hybridization in minority spin channel is observed between the Co_1、Co_2 and Ti atoms, as indicated by the arrows in Fig. 3(a). It gives rise to a large negative magnetic moment of -0.27 μ_B for Ti atom (see Table 1). It is due to the ferroelectrically displaced Ti atom approaches Co atom at the right much more than the value at the left interface($d_{Co-Ti,right} = 2.73$ Å and $d_{Co-Ti,\mathrm{left}} = 2.84$ Å). At the left interface, the weaker hybridization is observed between Co_1、Co_2 and Ti atoms in the minority spin channel, which leads to a small negative magnetic moment of -0.114 μ_B for Ti atom (see Table 1). (ii) In the $FeAl/TiO_2$ interface [see Fig. 3(b)], unoccupied Fe 3d state and Ti 3d state are well hybridized so that considerable Ti minority spin states appear close to Fermi energy E_F, resulting in a negative magnetic moment of Ti (see Table 1). This effect is enhanced at the right interface due to the relatively short bond length between Fe and Ti atoms($d_{Fe-Ti,right} = 2.91$ Å and $d_{Fe-Ti,\mathrm{left}} = 2.97$ Å), For either Co_2/TiO_2 or $FeAl/TiO_2$ interface, due to the small hybridization between Co 3d and O 2p states (not shown), the induced magnetic moments of the interfacial O atoms listed in table 1 are relatively small.

Figure 4 depicts the spin density difference for both Co_2/TiO_2 interface and $FeAl/TiO_2$ interface. The spin

density difference is obtained by subtracting the spin density of freestanding Co_2FeAl and $BaTiO_3$ slabs from the total spin density in the $Co_2FeAl/BaTiO_3$ MFTJ. For both Co_2/TiO_2 and $FeAl/TiO_2$ interfaces, from Fig. 4, it is clear that the charge distributions of Ti atoms at two interfaces have a character of the d_{xz} (d_{yz}) orbitals, which is similar to the result of $Fe/BaTiO_3/Fe$.[12] In $Co_2FeAl/BaTiO_3$ junction, the interfacial electrodes Co and Fe atoms bond with the O atoms. The spin charge transfer from Co and Fe atoms to Ti atoms via O atoms will occupy the d orbital of Ti atoms, which induces the magnetic moment of Ti atoms. The spin charge transfers between Co-Ti and Fe-Ti in the right interfaces are more than those in the left interface, which leads to the fact that the spin charge gained by the Ti atoms at right interface is greater than that at left interface. Therefore, the induced magnetic moment of Ti atom at right interface is larger than that at left interface by $0.156\mu_B$ and $0.15\mu_B$ for the Co_2/TiO_2 interface and $FeAl/TiO_2$ interface, respectively. The symmetry is broken due to the appearance of ferroelectricity in symmetry $Co_2FeAl/BaTiO_3$ MFTJ.

Finally, it is interesting to check the external strain effect on ME coupling in the $Co_2FeAl/BaTiO_3$ MFTJ, because recent works have suggested the external strain can enhance the ME coupling in MFTJs due to the strong interaction between the ME effect and the ferroelectric polarization.[50,51] So, we focus on the ferroelectricity polarization and ME coupling in $Co_2FeAl/BaTiO_3$ MFTJ with loaded biaxial in-plane strain in the x-y plane. Here, only the $FeAl/TiO_2$ interface is considered due to its larger magnetoelectric effect. Fig. 5 shows the relative Ti-O displacements of each TiO_2 atomic layer in the range of in-plane strain from -3% to 3%. For all the case, the $BaTiO_3$ side is divided into two regions with oppositely oriented polarization, but there is an overall net polarization. It can be seen that the increasing in-plane compressive strains lead to further increase of net polarization, and the tensile strains lead to further decrease of net polarization. It is consistent with the previous studies.[31,32] Therefore, the enhanced ferroelectricity of MFTJ can be implemented by using a substrate with small lattice parameters relative to that of $BaTiO_3$.

In order to understand how the interfacial magnetoelectric effect of the MFTJ is affected by the in-plane strain, we show the magnetic moments of interfacial Fe and Ti atoms in the MFTJ in Fig. 6. With further increase of in-plane compressive strain, the differences of the magnetic moments of Fe and Ti atoms between the two interfaces become larger and larger. For example, without the in-plane strain, the difference of the magnetic moments at the two interfaces is 0.032 μ_B for Fe atoms and 0.15 μ_B for Ti atoms. But when the loaded in-plane compressive strain increases to -3%, the difference of the magnetic moments is increased to 0.143 μ_B for Fe atoms and 0.293 μ_B for Ti atoms. The calculated magnetoelectric coefficient α_s of MFTJs increases correspondingly to $3.15\times10^{-10}\,\mathrm{Gcm^2/V}$ when the in-plane compressive strain reaches -3%, while $\alpha_s = 1.3\times10^{-10}\,\mathrm{Gcm^2/V}$ for the unstrained MFTJ. In contrast, the tensile strain leads to a smaller magnetoelectric coefficient. The result suggests that the magnetoelectric coupling in MFTJ can be enhanced by the in-plane compressive strain.

4. Conclusions

In summary, using first-principles calculations based on DFT, we have studied the critical thickness for ferroelectricity and ME effect at the $Co_2FeAl/BaTiO_3$ MFTJs. Our result shows that the critical thickness of ferroelectric state was about 1.7nm in $Co_2FeAl/BaTiO_3$ MFTJ for both Co_2/TiO_2 and $FeAl/TiO_2$ interfaces. And the ME coupling effects at these two interfaces are investigated. The interfacial electronic hybridization between unoccupied transition metal and Ti d states is mainly responsible for magnetoelectricity, similar to that previously reported for $Fe/BaTiO_3$. Compared with the Co_2/TiO_2 interface, a larger ME coefficient is achieved at the $FeAl/TiO_2$ interface, indicating that the ME coupling in $Co_2FeAl/BaTiO_3$ MFTJ can be modulated by the selection of the interfacial termination. In addition, we also find that the magnetoelectric coupling in MFTJ can be enhanced by the in-plane compressive strain.

Acknowledgements

The authors would like to acknowledge the National Natural Science Foundation of China Nos. 11274130,

11474113 and 11374111.

References

[1] M. Fiebig, J. Phys. D: Appl. Phys., 2005, 38, R123.

[2] N. A. Spaldin and M. Fiebig, Science, 2005, 309, 391.

[3] W. Eerenstein, N. D. Mathur and J. F. Scott, Nature, 2006, 442, 759.

[4] F. Manfred, J. Phys. D: Appl. Phys., 2005, 38, R123.

[5] J. D. Burton and E. Y. Tsymbal, Phil. Trans. R. Soc. A, 2012, 370, 4840.

[6] J. P. Velev, S. S. Jaswal and E. Y. Tsymbal, Phil. Trans. R. Soc. A, 2011, 369, 3069.

[7] C. A. Vaz, J. Phys.: Condens. Matter, 2012, 24, 333201.

[8] J. P. Velev, C. G. Duan, J. D. Burton, A. Smogunov, M. K. Niranjan, E. Tosatti, S. S. Jaswal and E. Y. Tsymbal, Nano Lett., 2009, 9, 427.

[9] D. Pantel, S. Goetze, D. Hesse and M. Alexe, Nature Mater., 2012, 11, 289.

[10] A. Petraru, H. Kohlstedt, U. Poppe, R. Waser, A. Solbach, U. Klemradt, J. Schubert, W. Zander, and N. A. Pertsev, Appl. Phys. Lett., 2008, 93, 072902.

[11] J. Junquera and P. Ghosez, Nature, 2003, 422, 506.

[12] C. G. Duan, S. S. Jaswal and E.Y. Tsymbal, Phys. Rev. Lett., 2006, 97, 047201.

[13] J. M. Rondinelli, M. Stengel and N. A. Spaldin, Nature Nanotechnol., 2008, 3, 46.

[14] D. Cao, M. Q. Cai, W. Y. Hu and C. M. Xu, J. Appl. Phys., 2011, 109, 114107.

[15] K.Yamauchi, B. Sanyal and S. Picozzi, Appl. Phys. Lett., 2007, 91, 062506.

[16] M. K. Niranjan, J. P. Velev, C. G. Duan, S. S. Jaswal and E.Y. Tsymbal, Phys. Rev. B, 2008, 78, 104405.

[17] J. F. Chen, C. S. Lin, Y. Yang, L. Hu and W. D. Cheng, Modelling Simul. Mater. Sci. Eng., 2014, 22, 015008.

[18] J. Q. Dai, H. Zhang and Y. M. Song, J. Magn. Magn. Mater., 2012, 324 , 3937.

[19] M. K. Niranjan, J. D. Burton, J. P. Velev, S. S. Jaswal and E.Y. Tsymbal, Appl. Phys. Lett., 2009, 95, 052501.

[20] Q. L. Fang, J. M. Zhang, K. W. Xu and V. Ji, Thin Solid Films, 2013, 540, 92.

[21] J. D. Burton and E.Y. Tsymbal, Phys. Rev. B, 2009, 80, 174406.

[22] L.Y. Chen, C. L. Chen, K. X. Jin, X. J. Du and A. Ali, J. Appl. Phys., 2013, 114, 144101.

[23] H. J. A. Molegraaf, J. Hoffman, C. A. F. Vaz, S. Gariglio, D. D. Marel, C.H. Ahn and J. M. Triscone, Adv. Mater., 2009, 21, 3470.

[24] X. T. Liu, Y. Zheng, B. Wang and W. J. Chen, Appl. Phys. Lett., 2013, 102, 152906.

[25] D. Cao, B. Liu, H. L. Yu, W. Y. Hu, M. Q. Ca, Eur. Phys. J. B, 2013, 86, 504.

[26] B. L. Yin and S. X. Qu, Phys. Rev. B, 2014, 89, 014106.

[27] J. Q. Dai, Y. M. Song and H. Zhang, J. Magn. Magn. Mater., 2014, 354, 299.

[28] W. Eerenstein, N. D. Mathur and J. F. Scott, Nature , 2006, 442, 759.

[29] C. Thiele, K. Dörr, O. Bilani, J. Rödel and L. Schultz. Phys. Rev. B, 2007, 75, 054408.

[30] F. Hao, Y. M. Pei and D. N. Fang，J. Appl. Phys., 2013, 114, 044109.

[31] O. Diéguez, K. M. Rabe and D. Vanderbilt, Phys. Rev. B, 2005, 72, 144101.

[32] K. J. Choi, M. Biegalski, Y. L. Li,A. Sharan, J. Schubert, R. Uecker, P. Reiche, Y. B. Chen, X. Q. Pan,V. Gopalan, L. Q. Chen, D. G. Schlom and C. B. Eom, Science, 2004, 306, 1005.

[33] H. J. Elmers, S. Wurmehl, G. H. Fecher, G. Jakob, C. Felser and G. Schönhense, J. Magn. Magn. Mater., 2004, 272, 758.

[34] W. Wang, E. Liu, M. Kodzuka, H. Sukegawa, M. Wojcik, E. Jedryka, G. H. Wu, K. Inomata, S. Mitani and K. Hono, Phys. Rev. B, 2010, 81, 140402.

[35] W. H. Wang, H. Sukegawa, R. Shan, S. Mitani and K. Inomata, Appl. Phys. Lett., 2009, 95, 182502.

[36] S. Qiao, S. H. Nie, J. H. Zhao, Y. Huo, Y. Z. Wu and X. H. Zhang, Appl. Phys. Lett., 2013, 103, 152402.

[37] H. C. Yuan, S. H. Nie, T. P. Ma, Z. Zhang, Z. Zheng, Z. H. Chen, Y. Z. Wu, J. H. Zhao, H. B. Zhao and L.Y. Chen, Appl. Phys. Lett., 2014, 105, 072413.

[38] S. Qiao, S. H. Nie, J. H. Zhao and X. H. Zhang, J. Appl. Phys., 2013, 113, 233914.

[39] G. Kresse and J. Furthmüller, Phys. Rev. B, 1996, 54, 11169.

[40] G. Kresse and D. Joubert, Phys. Rev. B, 1999, 59, 1758.

[41] J. P. Perdew, K. Burke and M. Ernzerhof. Phys. Rev. Lett., 1996, 77, 3865.

[42] X. G. Xu, D. L. Zhang, W. Wang, Y. Wu, Y. K. Wang and Y. Jiang, J. Magn. Magn. Mater., 2010, 322, 3351.

[43] H. J. Monkhorst and J. D. Pack, Phys. Rev. B, 1976, 13, 5188.

[44] I. I. Oleinik, E. Y. Tsymbal and D. G. Pettifor, Phys. Rev. B, 2001, 65, 020401(R).

[45] G. H. Kwei, A. C. Lawson and S. J. L. Billinge, J. Phys. Chem. 1993, 97, 2368.

[46] R. D. King-Smith and D. Vanderbilt, Phys. Rev. B, 1993, 47, 1651.

[47] I. Galanakis, P. H. Dederichs and N. Papanikolaou, Phys. Rev. B, 2002, 66, 174429.

[48] R. R. Mehta, B. D. Silverma and J. T. Jacobs, J. Appl. Phys. 1973, 44, 3379.

[49] M. K. Niranjan, J. D. Burton, J. P. Velev, S. S. Jaswal and E.Y. Tsymbal, Appl. Phys. Lett., 2009, 95, 052501.

[50] D. Cao, H. B Shu, Z. W. Jiao, Y. Zhou, M. G Chen, M. Q Cai and W. Y Hu. Phys. Chem. Chem. Phys., 2013, 15, 14770.

[51] Z. G. Wang, Y. J. Wang, H. S. Luo, J. F. Li and D. Viehland, Phys. Rev. B, 2014, 90, 134103.

Table 1

Magnetic moments in μ_B of the atoms at the left and right interfaces in the $Co_2FeAl/BaTiO_3$ junction. $\mu(I_L)$ ($\mu(I_R)$) is the magnetic moment of the atom at the left (right) interface. $\mu(\text{Middle})$ is the magnetic moment of the atom at the middle layer between the interfaces. And $\Delta\mu(I_L - I_R)$ denotes the difference between the magnetic moments at the right and left interfaces. The FE polarization of $BaTiO_3$ is pointing rightward (see Fig. 1.)

Interface	Atom	$\mu(\text{Middle})$	$\mu(I_L)$	$\mu(I_R)$	$\Delta\mu(I_L - I_R)$
Co_2/TiO_2	Co_1	1.225	1.771	1.782	-0.011
	Co_2	1.242	1.825	1.833	-0.008
	Ti	0.001	-0.114	-0.270	0.156
	O_1	0.000	0.043	0.049	-0.006
	O_2	0.000	0.053	0.063	-0.010
$FeAl/TiO_2$	Fe	3.057	3.173	3.141	0.032
	Al	-0.053	-0.036	-0.038	0.002
	Ti	0.003	-0.107	-0.257	0.150
	O_1	0.000	-0.007	-0.004	-0.003
	O_2	0.000	0.037	0.037	0.000

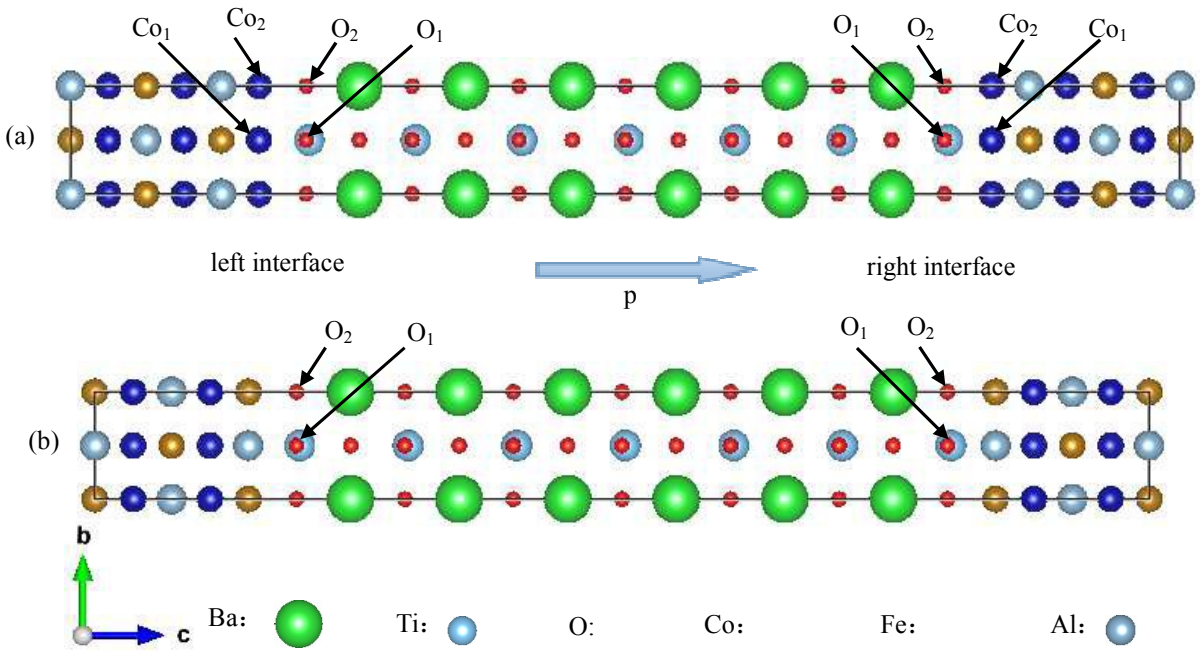

Fig. 1. Ball and stick model of $Co_2FeAl/BaTiO_3/Co_2FeAl$ junction with (a) Co_2/TiO_2 and (b) $FeAl/TiO_2$ interface. The solid arrow denotes the direction of polarization in $BaTiO_3$.

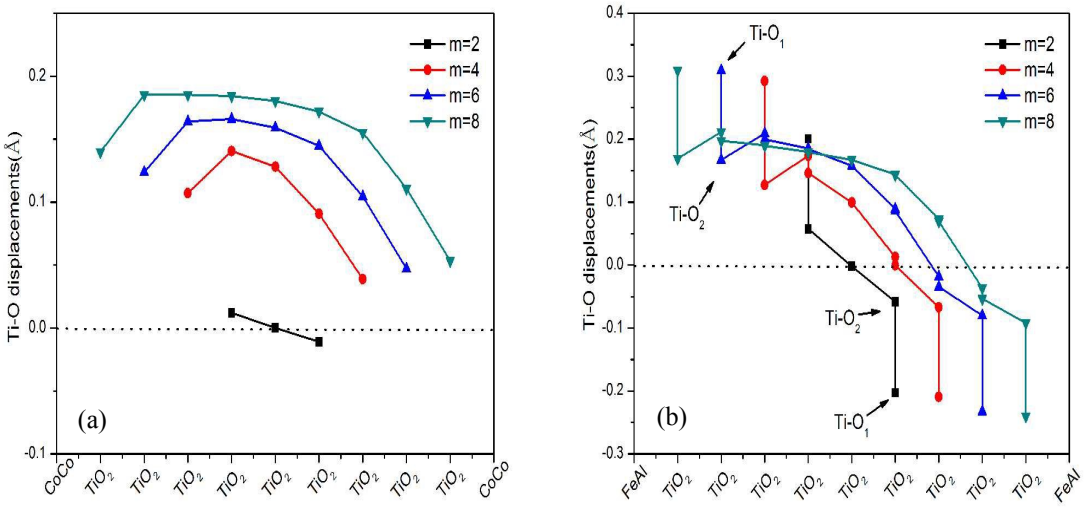

Fig. 2. The relative Ti-O displacements within each atomic layer of different $BaTiO_3$ layers in $Co_2FeAl/BaTiO_3/Co_2FeAl$ junction with (a) Co_2/TiO_2 and (b) $FeAl/TiO_2$ interface. The positive value denotes the electric dipole moment of Ti-O pointing to the right, which is the same as the direction of polarization. For (b) $FeAl/TiO_2$ interface, the O_1 and O_2 represent the O atoms which terminate with the interfacial Al and Fe atoms, respectively.

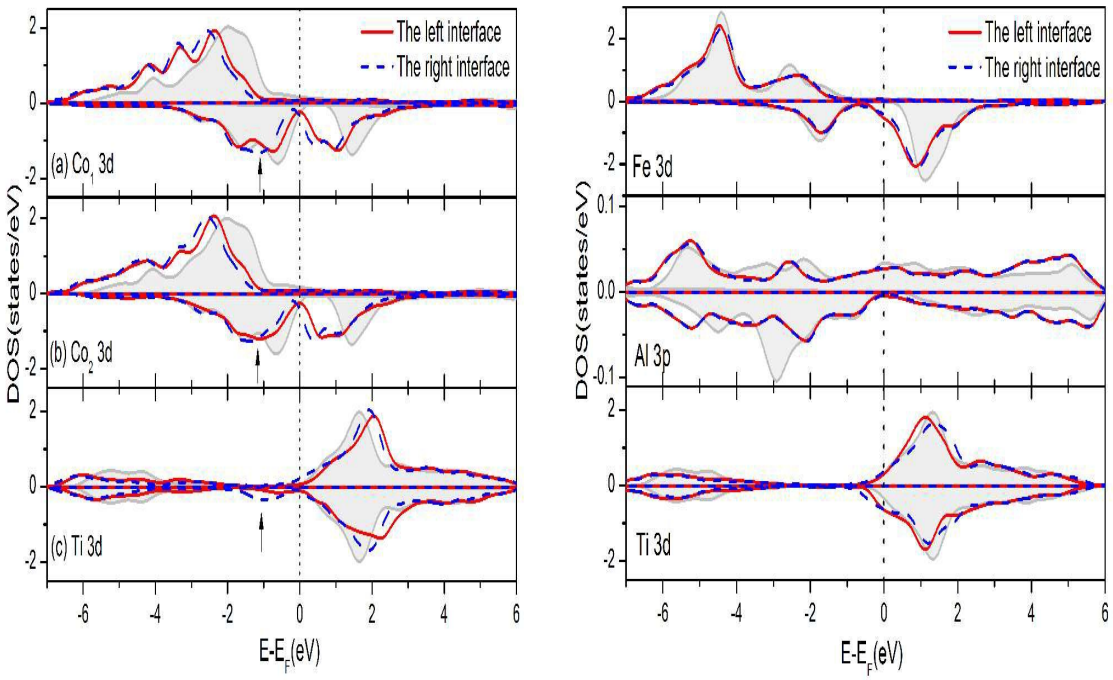

Fig. 3. The PDOS for the left (the solid red lines) and right (the dashed blue lines) interfacial atoms in the $Co_2FeAl/BaTiO_3$ (m=6) junction with (a) Co_2/TiO_2 and (b) $FeSi/TiO_2$ interface, respectively. The shaded plots correspond to the DOS of atoms in the center layer which are similar to the DOS in bulk. The DOS of majority spin and minority spin are plotted in the upper and lower panels. The dashed vertical line indicates the Fermi energy.

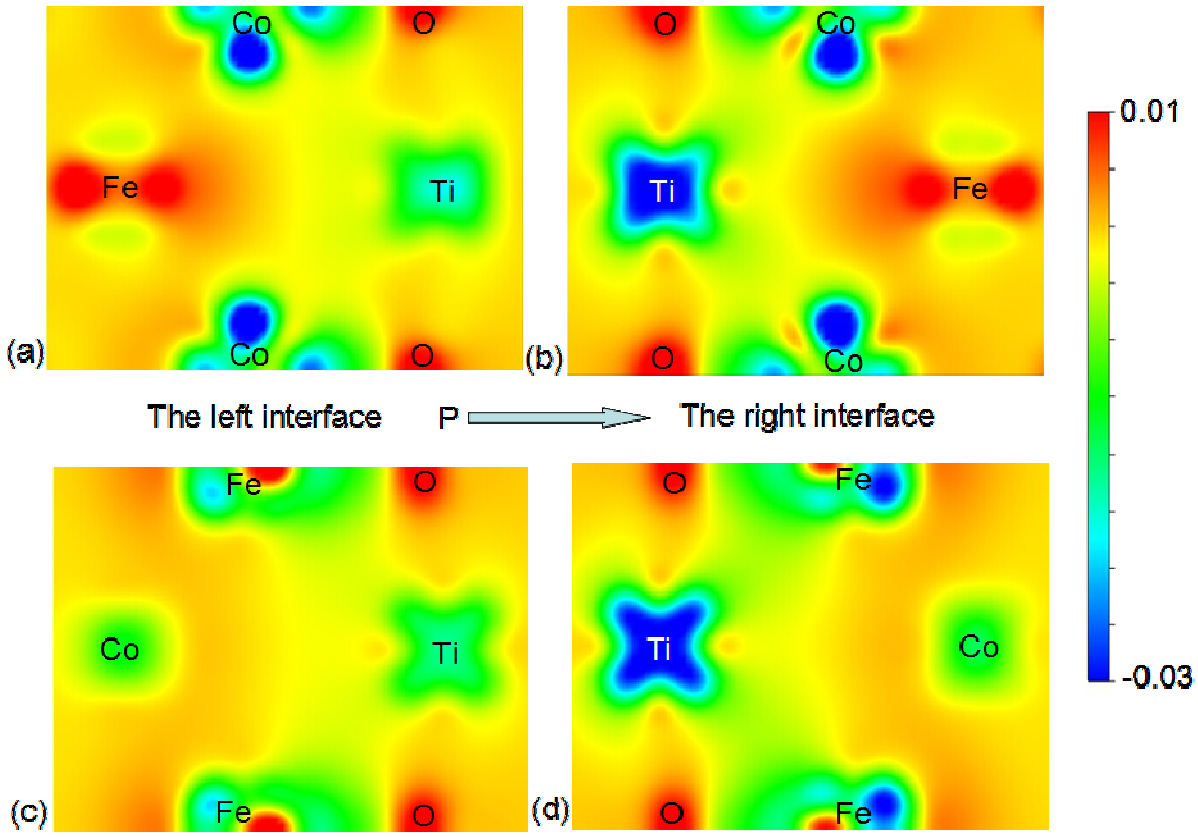

Fig. 4. the spin density difference at the left and right interfaces for (a), (b) the Co_2/TiO_2 termination and (c), (d) the $FeAl/TiO_2$ termination in $Co_2FeAl/BaTiO_3$ (m=6) tunnel junctions. The arrow denotes the direction of FE polarization: from the left interface to the right interface (the same as in Fig. 1). Color scales are in units of e $Å^{-3}$.

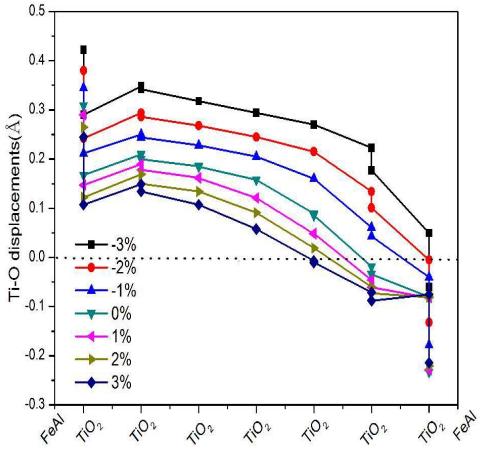

Fig. 5 The relative Ti-O displacements of each Ti-O atomic layer in the $BaTiO_3$ multilayers in $Co_2FeAl/BaTiO_3$ MFTJ with different in-plane strain for the $FeAl/TiO_2$ termination.

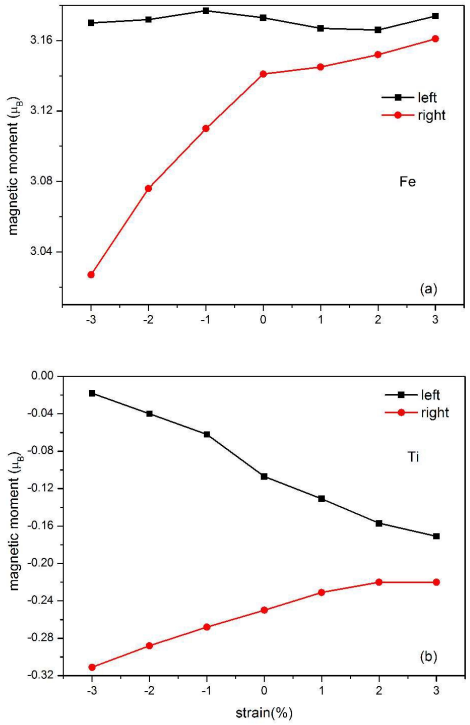

Fig. 6 The magnetic moments (μ_B) of (a) Fe and (b) Ti atoms at the left and right interfaces of $Co_2FeAl/BaTiO_3$ MFTJ with different in-plane strains for the $FeAl/TiO_2$ termination.